

Copyright © 1990, by the author(s).
All rights reserved.

Permission to make digital or hard copies of all or part of this work for personal or classroom use is granted without fee provided that copies are not made or distributed for profit or commercial advantage and that copies bear this notice and the full citation on the first page. To copy otherwise, to republish, to post on servers or to redistribute to lists, requires prior specific permission.

**KINETICS OF PHOTORESIST ETCHING
IN AN ELECTRON CYCLOTRON
RESONANCE PLASMA**

by

D. A. Carl, D. W. Hess, and M. A. Lieberman

Memorandum No. UCB/ERL M90/25

3 April 1990

**KINETICS OF PHOTORESIST ETCHING
IN AN ELECTRON CYCLOTRON
RESONANCE PLASMA**

by

D. A. Carl, D. W. Hess, and M. A. Lieberman

Memorandum No. UCB/ERL M90/25

3 April 1990

ELECTRONICS RESEARCH LABORATORY

College of Engineering
University of California, Berkeley
94720

**KINETICS OF PHOTORESIST ETCHING
IN AN ELECTRON CYCLOTRON
RESONANCE PLASMA**

by

D. A. Carl, D. W. Hess, and M. A. Lieberman

Memorandum No. UCB/ERL M90/25

3 April 1990

ELECTRONICS RESEARCH LABORATORY

College of Engineering
University of California, Berkeley
94720

Kinetics of photoresist etching in an electron cyclotron resonance plasma

D. A. Carl and D. W. Hess (Department of Chemical Engineering)
and
M. A. Lieberman (Department of Electrical Engineering and Computer Sciences)

University of California
Berkeley, CA 94720
(415) 642-2483

ABSTRACT

An electron cyclotron resonance (ECR) plasma processing system was used to etch hardbaked KTI820 photoresist from single crystal silicon wafers, silicon dioxide films and patterned multilayer structures. Etch rates of 1500 nm/minute were observed at a substrate temperature below 373 K in a $P_{\text{forward}} = 750$ W, 0.13 Pa ECR oxygen plasma with no applied substrate bias. The etch rate increased linearly with increasing power from $P_{\text{forward}} = 300$ to 750 W. Etch rate was a complicated function of pressure and residence time, but a modified adsorption--reaction--ion-stimulated desorption rate expression could be used to fit the data. Etch rates decreased for increasing oxygen residence time at low operating pressures due to a combination of polymeric film formation of reaction products and reactant (atomic oxygen) depletion. Maximum etch rates were observed at approximately 0.13 Pa for all residence times. Multilayer photoresist structures were etched at various pressures as well as at a 45° angle to the incident plasma stream. Etch profiles for the variable angle runs indicated that the etch rate was strongly dependent on ion flux. Etch anisotropy increased with decreasing pressure, consistent with increased ion bombardment energy. The degree of anisotropy was, however, limited due to a non-normal component of ion energy, which has been interpreted previously as an ion temperature.

I. INTRODUCTION

Oxygen plasmas have long been used to remove residual photoresist from process wafers in the microelectronics industry.¹ With the introduction of submicron features in integrated circuits much effort has been expended to formulate dry development and patterning methods for photoresist layers.^{1,2} Toward this goal, investigations of possible photoresist etch mechanisms of oxygen and oxygen-containing plasmas have been performed.¹⁻⁴ Although atomic oxygen is generally considered to be the primary etchant specie, the exact dependence of the etch rate on oxygen concentration can be complicated. In addition, ion flux and ion energy significantly affect etch rate, but, although models have been proposed, the exact etch rate dependence is not well understood.⁴

In this study, the effects of power, pressure, temperature, flow rate (residence time of etchant), dilution of etchant, and wafer angle to the plasma flux on the etch rate of hardbaked KTI 820 photoresist and upon the profiles of multilayer structures etched in an ECR oxygen plasma with a mirror magnetic field were examined. No external bias was applied to the wafer during these experiments. The etch rate behavior in this system was then analyzed in light of the photoresist etching model proposed by Joubert *et al.*⁴

II. EXPERIMENTAL

The ECR system used in these experiments has been described previously.⁵ A 2.45 GHz, 800 W CW microwave power supply/matching network was connected by a WR284 rectangular waveguide and a quartz window to the cylindrical vacuum chamber. No special microwave mode conversion was used. Two and three inch silicon wafers with 1 to 1.5 μm (as measured by a Nanospec Thin Film measurement system) of hardbaked KTI820 photoresist were clamped onto an aluminum holder via a retention ring. The temperature of the holder assembly was monitored with a thermocouple. An MKS 247 mass flow control unit attached to three MKS 1259B mass flow controllers was used in conjunction with an MKS 390 pressure measurement system to control etchant gas flow rate (from 2 to 40 sccm) and system pressure. Oxygen residence times were calculated based upon a reactor volume of 7990 cm^3 and inlet flow conditions.

Optical emission spectroscopy (OES) (Plasma Therm PSS-2) was used to monitor the photoemission intensities of etchant and product species prior to and during the etch sequence. OES was used for etch

endpoint detection by monitoring the 519 nm CO or the 656 nm H emission line. Both lines were accurate endpoint monitors. The endpoint detection method was calibrated by performing partial etches at a representative set of conditions and measuring final film thickness. The thickness of film removed was divided by the etch time to yield etch rate. It was assumed that the etch rate was constant over the etch interval. OES was also used to perform actinometry using the 750.4 nm Ar emission line as a reference. A Langmuir probe was used to determine the ion density (n_i), electron temperature (T_e), ion current (j) and ion energy (E_i) as functions of the parameter space investigated. Scanning electron microscopy (SEM) was used to analyze etch profiles of multilayer photoresist structures.

III. RESULTS AND DISCUSSION

A. Discharge Characteristics

Langmuir probing was used to determine plasma electrical parameters over a wide range of external conditions by the method of Laframboise.⁶ The ion density measured at the wafer was linear with power from $P_{\text{forward}} = 150$ to 750. Maximum oxygen ion (O_2^+ and O^+) density was exhibited when the magnet coil current was 150 A, which corresponded to resonance at the magnetic mirror midplane in the system source chamber.⁵ Since the photoresist etch rate was a strong function of n_i via j , these experiments were performed with 150 A coil current. The effect of pressure on n_i and T_e at constant ECR power absorbed is shown in Fig. 1. The electron temperature exhibited a strong pressure dependence, increasing nearly logarithmically as pressure decreased. The ion density increased rapidly from 0.03 to 0.13 Pa and exhibited a maximum at ≈ 0.13 Pa, the same pressure where maximum etch rate was observed. This variation of n_i with pressure has been observed in other ECR discharges.⁷ From the information contained in Fig. 1, the ion current to the wafer can be calculated as a function of system pressure using the Bohm flux relation:⁸

$$j = 0.6en_i \left(\frac{eT_e}{M_i} \right)^{1/2} \quad [1]$$

where M_i is the mass of the ion. Fig. 2 shows the ion current (j) to the wafer as a function of pressure. In agreement with the ion density dependence on pressure, j increased sharply with increasing pressure from 0.03 Pa to ≈ 0.13 Pa, decreasing below this pressure.

The photoemission intensities for several O_2^+ , O^+ , and atomic oxygen transitions are consistent with previous studies.⁹ Since the ionic emissions track n_i , these signals were used as a non-intrusive tuning monitor. Most of the atomic transitions showed similar behavior, rising linearly with increasing power, i.e., with increasing n_i and therefore with electron density, n_e . As emission intensities are complicated functions of T_e , n_i and the concentrations of various oxygen species, concentrations of product and reactant species cannot be quantitatively determined in the present system. However, a relative measure of atomic oxygen concentration compared to a reference condition was obtained using actinometry. The ratio of optical emission signal intensity of the 844.5 nm O line to the 750.4 nm Ar line has been shown to be an accurate measure of the concentration ratios of the two species at low pressure.¹⁰ Fig. 3 shows relative atomic oxygen concentration ($[O]$) versus pressure, as referenced to $[O]$ at 0.13 Pa. Atomic oxygen concentration is linear with increasing O_2 pressure up to 1.3 Pa. Relative concentration appears to saturate at a level of ≈ 7 times the concentration at 0.13 Pa over the pressure range 1.3 to 6 Pa. This saturation is probably due to the combination of increasing oxygen concentration (due to increasing pressure), decreasing T_e (thus decreasing the rate constants for the various dissociation processes), and decreasing n_e (therefore decreasing the overall dissociation rate as pressure increases). The same technique was used to show that the relative $[O]$ was linearly proportional to the partial pressure of O_2 in the inlet feed stream in gas mixtures of CO and N_2 . This result has been observed previously under similar conditions and is consistent with the fact that the measured n_i and T_e do not change appreciably as a function of gas composition under these plasma conditions.⁴

B. Etch Rate Observations

Fig. 4 shows the etch rate of KTI 820 photoresist as a function of both pressure and residence time of the inlet O_2 . Etch rate is clearly a complicated, non-linear function of both residence time and pressure. In order to explain these data, the proposed etch mechanism and its dependence upon measured or calculated parameters must be reviewed.

1. Proposed Model

Joubert *et al* have recently proposed a model for oxygen plasma etching of polymers.⁴ The form of the proposed rate expression is:

$$r = \frac{k_1 (\kappa p_o) \langle \eta \sigma_s \rangle j}{(\kappa p_o) + \langle \eta \sigma_s \rangle j} \quad [2]$$

where r is the rate of reaction, k_1 is the rate coefficient, p_o is the atomic oxygen partial pressure in the system, κ is the thermodynamic adsorption constant for atomic oxygen, σ_s is the density of adsorption sites for atomic oxygen, and η is the ion induced desorption rate constant which includes effects for desorption and stoichiometry of etch products. The rate constant η is assumed to be an unknown function of ion bombardment energy, E_i , and of ion bombardment angle. This mechanism can be viewed as a sum of series resistances to the etch process. For such an expression, a linear relationship between the etch rate and a particular variable (p_o or j) is observed for small values of that variable, whereas saturation is observed for large values of the variable.⁴ In order to obtain values for the constants in Eqn. [2], all conditions but one must be held constant and the variation of r with this parameter examined.

Extracting the values of each individual constant of Eqn. [2] requires information that could not be measured with our experimental apparatus. It was possible, however, to isolate and extract the values of two groups of these variables with the data acquired from actinometry, Langmuir probe studies, and specific etch rate experiments. Actinometric data confirmed that the partial pressure of O can be linearly related to the O_2 concentration in the plasma for constant T_e and n_i (i.e. constant power and total pressure) for O_2 , CO and N_2 mixtures. Therefore, p_o can be redefined as ($p_{o,ref} x$), where x is the mole fraction of O_2 in the plasma. (It should be noted that x is generally not the mole fraction of the inlet gas feed, due to the creation of etch product gases and dissociation into atomic oxygen. x can be estimated using a simple continuous stirred tank reactor model and a material balance upon the CO, H_2O and O in the system. Under "worst case" conditions (0.13 Pa and 213 ms residence time) [O] was at least 25% of [O_2]) It is convenient to rearrange Eqn. [2] into the following form:

$$\frac{x}{r} = \frac{x}{k_1 \alpha_2} + \frac{1}{k_1 \alpha_1} \quad [3]$$

where α_1 is the product ($\kappa p_{O,ref}$) and α_2 is the product $\langle \eta \sigma_s j \rangle$. As the Langmuir probe data indicated that T_e and n_i were essentially constant (thus j was constant via Eqn.[1]) for various mixtures of O_2 , CO, N_2 and Ar, the α_2 term should be constant for constant total pressure. Fig. 5 shows a series of etches which were performed at constant total pressure (0.13 Pa), power (550 W) and residence time (72 ms) with mixtures of N_2 , Ar, and CO with O_2 . The 0.13 Pa etch rates with CO mixtures were clearly quite different from the Ar and N_2 mixes. If it is assumed that O_2 -CO mixtures can form carbonaceous deposits as well as etch the original film, then Eqn.[2] can be modified to:

$$r_t = r_o - r_d \quad [4]$$

where r_t is the modified etch rate, r_o is the rate as predicted by Eqn. [3], and r_d is the deposition rate of the film. To a first approximation, the deposition rate should be proportional to the gas phase CO concentration. A blanket film deposition process should not be selective with respect to specific surface sites: thus a site-balance model similar to the one used to generate Eqn. [1] is not appropriate. The above also assumes that the film being deposited is similar to the film being etched and thus can be etched by the same mechanism of Eqn. [1]. Therefore, we assume that r_d has the form:

$$r_d = k_2 P_{total} x_{CO} \quad [5]$$

where k_2 is the rate constant for deposition, p_{total} is the total pressure, and x_{CO} is the CO mole fraction. Since there is a significant fraction of CO ($\approx 25\%$ at pure O_2 feed) in the reactor under these conditions, an iterative process must be used to extract the constants in Eqns. [3] and [5] in order to ensure consistency. This regression yields values of $0.15 \text{ min } \mu\text{m}^{-1}$ for $1/(k_1 \alpha_2)$, $0.342 \text{ min } \mu\text{m}^{-1}$ for $1/(k_1 \alpha_1)$ and $3.37 \mu\text{m min}^{-1} \text{ Pa}^{-1}$. Fig. 5 shows the fit to data using these constants.

The 0.13 Pa reference values for the constants in Eqns. [1] - [4], the actinometric p_o vs. pressure, and the j vs. pressure data can now be combined to form the overall etch rate expression:

$$r_i = \frac{x}{\frac{x}{k_1 \alpha_2} \left(\frac{j_o}{j} \right) \left(\frac{\eta_o}{\eta} \right) + \frac{1}{k_1 \alpha_1} \left(\frac{p_o}{p} \right)} - k_2 P_{total} x_{CO} \quad [6]$$

This expression has one variable parameter-- η_o/η (the relative cross section for ion induced desorption)--which should be a strong function of E_i . If Eqn. [6] is valid, a set of constant residence time etch rate vs. pressure curves can be used to regress the functional dependence of η/η_o vs. pressure, and thus E_i as shown below. This functionality can then be substituted back into Eqn. [6] and determined at different residence times (i.e., at different x and x_{CO}).

2. Power, Pressure and Residence Time

Etch rate increased linearly with increasing power from $P_{forward} = 150$ to 700 W at constant pressure; no etch rate saturation with power was observed. Fig. 6 shows etch rate as a function of pressure for 72 ms, 142 ms and 213 ms oxygen residence times, and the predicted rate from Eqn. [6], with appropriate substitutions for p_o and j as functions of pressure and with η/η_o determined from the 72 ms data. Eqn. [6] predicts a somewhat lower rate than that observed for both the 142 ms and the 213 ms residence time cases, but does predict the general trend. A material balance on oxygen indicates that the etch reaction is supply-limited at such pressures and high etchant residence times. Indeed, when the etch sample (photoresist) area was varied at 213 ms residence time, 0.13 Pa, and 550 W, the etch rate was linear with the reciprocal of the resist area. This type of classical loading effect has been described previously.¹¹ As pressure was increased, the residence time/loading effect decreased; no loading effect was observed at pressures above ≈ 2 Pa. Eqn. [6] predicts this general behavior due to its sensitivity to x .

The relationship between E_i and pressure must be established to assess the validity of the η/η_o vs. E_i correlation. As the sample holder was electrically floating in the plasma, an estimate of ion energy can be made by assuming that the ions fall through two effective sheaths; a distributed sheath due to ion density variations along the axis of the ECR plasma, and the normal sheath found at the plasma-wafer interface. The potential drop across the distributed sheath due to Boltzmann equilibrium for the electrons can be expressed as:

$$\Delta V_1 = \frac{kT_e}{e} \ln \left(\frac{n_{i,o}}{n_{i,wafer}} \right) \quad [7]$$

where $(n_{i,o}/n_{i,wafer})$ is the ratio of ion density in the ECR zone to the density at the wafer. This ratio was found to be approximately 10 in our ECR system. The potential drop across the normal sheath can be estimated from the Bohm sheath relation:

$$\Delta V_2 = 0.5 \frac{kT_e}{e} \ln \left(\frac{8M_i}{\pi m} \right) \quad [8]$$

where m is the electron mass. Thus E_i , which is the sum of the two potential drops defined in Eqns. [7] and [8], can be estimated for various pressures from the data in Fig. 1. Fig. 7 shows η/η_0 vs. E_i . This curve exhibits an apparent threshold energy of ≈ 20 V. This value is comparable to sputtering thresholds.¹² As E_i values were relatively small in the experiment, no saturation with energy was observed for this η . Therefore, although a direct measurement of the dependence of η on E_i could not be made in this system, the form obtained indirectly is consistent with other physical sputtering phenomena.

3. Angle of Wafer Relative to Plasma

The wafer holder on this ECR system can be rotated with respect to the plasma. Etch rates were measured at 0.13 Pa, 72 ms residence time, and $P_{\text{forward}} = 550$ W at various angles to the plasma stream. Fig. 8 shows etch rate vs. angle between the sample and the plasma flux, a cosine fit to the data, and a fit based upon substitution of a cosine dependence of j into Eqn. [6]. In this experiment, the primary etchant species (atomic oxygen) concentration was assumed to be relatively constant; but the ion flux varied as the wafer was rotated with respect to the plasma stream. The predicted angular dependence from Eqn. [6] is greater than the observed rate. This may be due to the fact that η is not only a function of E_i , but also of the angle of incidence of the impinging ion.

Pre-patterned and partially etched multilayer structures were etched at 45° to the plasma stream at 0.13 Pa, $P_{\text{forward}} = 550$ W and 72 ms residence time. The multilayer structures consisted of a 100 nm silicon

dioxide patterned mask on top of 1.1 μm of hardbaked photoresist. The photoresist was anisotropically etched to a depth of approximately 0.5 μm in parallel plate 13.56 MHz reactor prior to processing in the ECR oxygen plasma. The resulting cross-sectional profile and SEM photomicrograph are shown in Fig. 9. The effective angle of incidence of the incoming ion stream is less than 45° due to diffraction in the sheath.¹³ The sharp angle observed in the right sidewall/trench bottom interface of the structure is most likely due to a shadowing of ion flux from the top dielectric mask. Little if any etching is observed on the shadowed portion of the right sidewall. The apparent isotropic profile on the left hand side could be due to shadowing from the left-hand side dielectric mask or due to non-normal ion energy (referred to as ion temperature)¹⁴. SEM analysis of other structures on this test pattern indicated that the degree of anisotropy increased with decreasing pressure. Thus, anisotropy (5:1 or greater vertical:horizontal etch rate) can be achieved without external substrate bias, but at the cost of reduced etch rate.

4. Temperature Effects

Etching was performed on silicon wafers coated with 1.0 to 1.5 μm of photoresist under identical P_{forward} , pressure, and residence time conditions at temperatures from 300 K to 390 K with no measurable effect on etch rate. Wafers were thermally isolated from the substrate holder by placing small area silicon spacers between the wafer and the substrate holder with no measurable effect on etch rate. Furthermore, there was no difference in etch rate between samples of photoresist spun on oxidized wafers and those spun on bare silicon. Two explanations can be proposed for these observations: 1) the photoresist film heats rapidly due to plasma flux (photonic and ionic) heating and the heat of reaction; thus external temperature effects are masked; or 2) the activation energy for this process is negligible under these conditions. Thermal activation energies on the order of 8 to 10 kcal/mol have been reported previously for various photoresist stripping processes.¹⁵ With a high fluence of ions and energetic photons, surface and near surface bond breakage could be enhanced, thus promoting reaction and masking any temperature effect on the etch rate. Therefore k_1 in Eqn. [2] appears to be independent of temperature in the parameter space investigated.

IV. CONCLUSIONS

Hardbaked KTI 820 photoresist etch rate was investigated in an ECR plasma reactor as a function

of pressure, gas mixture, power, temperature, angle to the plasma stream and residence time. The rate was linear with power for $P_{\text{forward}} > 150$ W. A measured effective activation energy of essentially zero indicated that either the etch mechanism is initiated or controlled by ion or photon flux or that temperature effects are masked by plasma heating of the photoresist film. Etch rate was a complicated function of pressure and residence time for a fixed power, but could be modeled by an adsorption--reaction--ion-stimulated desorption process with simultaneous polymeric film deposition. Etch rates decreased with increasing residence time for all pressures and powers with the effect most prominent at low pressure. SEM analysis of multilayer structures demonstrated the dependence of etch rate on ion flux and indicated that the degree of anisotropy increased as pressure decreased.

ACKNOWLEDGMENTS

This work was supported by National Science Foundation Grant Nos. ECS-8517363 and ENG-8710988, Department of Energy Grant No. DE-FG03-87ER13727, and a contract from IBM General Technology Div., Burlington, VT. The authors would like to thank W. Mlynko of IBM for providing the multilayer resist structures, S. Savas and D. Flamm for helpful discussions on proper actinometry technique and R. Wilson of the Material Science and Mineral Engineering Department of the University of California for assistance with the SEM photographs.

REFERENCES

1. M. A. Hartney, D. W. Hess and D. S. Soane, J. Vac. Sci. Tech. B 7,1 (1989) and references within.
2. J. E. Heidenreich, J. R. Paraszczak, M. Moisan and G. Sauve, Micro. Eng. 5, 363 (1986).
3. S. Dzioba, G. Este and H. M. Naguib, J. Electrochem. Soc. 129, 2537 (1982).
4. O. Joubert, J. Pelletier and Y. Arnal, J. Appl. Phys. 65, 5096 (1989).
5. D. A. Carl, D. W. Hess and M. A. Lieberman, J. Vac. Sci. Tech. A, May/June (1990).
6. J. G. Laframboise, Inst. for Aero. Stud., Univ. of Toronto, Rep. No. 100 (1966).
7. S. Gorbatkin, J. Vac. Sci. Tech. A, May/Jun (1990).
8. F. F. Chen, Introduction to Plasma Physics and Controlled Fusion, Plenum Press, 296 (1985).
9. S. Kimura, E. Murakami, K. Miyake, T. Warabisako, H. Sunami and T. Tokuyama, J. Electrochem. Soc. 132, 1460 (1985).
10. R. Walkup, K. Saenger, and G. S. Selwyn, Mat. Res. Soc. Symp. Proc. 38, 69 (1985).
11. C. J. Mogab, J. Electrochem. Soc. 124, 1262 (1977).
12. R. V. Stuart and G. K. Wehner, J. Appl. Phys. 33, 2345 (1962).
13. T. Ono, M. Oda, C. Takahashi and S. Matsuo, J. Vac. Sci. Tech. B 4, 696 (1986).
14. W. M. Holber, J. Vac. Sci. Tech. A, May/Jun (1990).
15. C. W. Jurgensen and A. Rammelsberg, J. Vac. Sci. Tech. A 7, 3317 (1989).

FIGURE CAPTIONS

- Fig. 1: Plot of n_i and T_e vs. pressure. n_i and T_e were insensitive to oxygen residence time effects; n_i was linearly proportional to power at constant pressure while T_e was essentially constant vs. power.
- Fig. 2: Plot of j vs. pressure.
- Fig. 3: Plot of relative oxygen concentration vs. pressure.
- Fig. 4: Plot of etch rate vs. pressure and oxygen residence time for $P_{\text{forward}} = 550$ W and 150 A coil current.
- Fig. 5: Plots of etch rate and (x/r) vs. O_2 percentage in the reactor and r vs. O_2 percentage in the inlet stream mixtures with Ar, N_2 , and CO at 0.13 Pa, $P_{\text{forward}} = 550$ W and 150 A coil current. The fit from Eqns. [3] and [5] are shown as a solid line for the Ar and N_2 mixes; the CO mix fit is shown as the dashed line.
- Fig. 6: Plots of etch rate vs. pressure and residence times for the 72, 142 and 213 ms residence time cases. The fits are from Eqn. [6].
- Fig. 7: Plot of variation of the rate constant for ion induced desorption relative to the rate constant at 0.13 Pa (η/η_0) with ion energy.
- Fig. 8: Plot of the etch rate vs. angle at $P_{\text{forward}} = 550$ W and 150 A coil current. 90° is normal incidence.
- Fig. 9: SEM photomicrograph and diagram of multilevel photoresist structure etched at a 45° to the plasma stream. The ion stream is partially diffracted by the sheath and subsequently the actual angle of incidence at the structure is less than 45° .

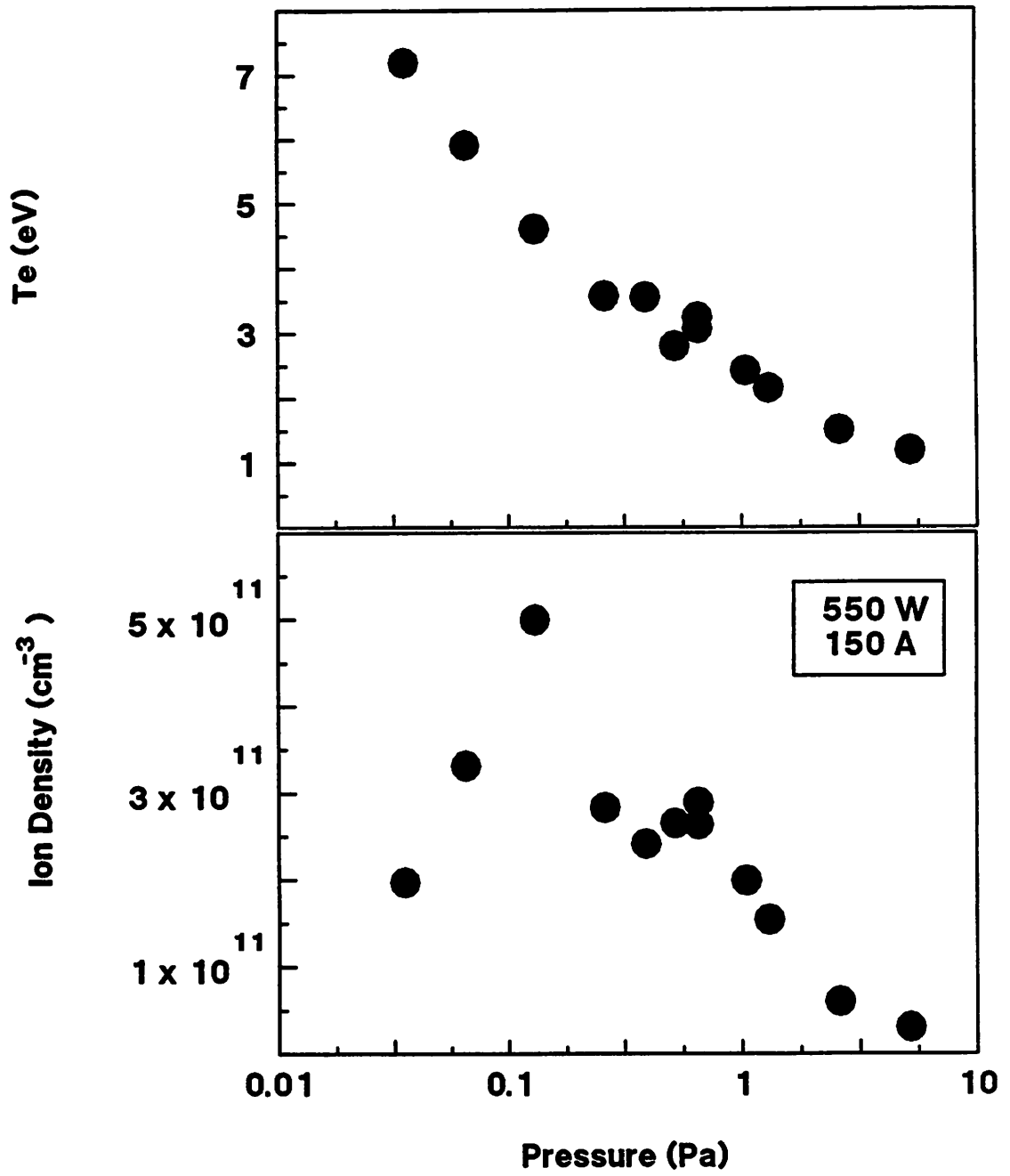


Fig. 1

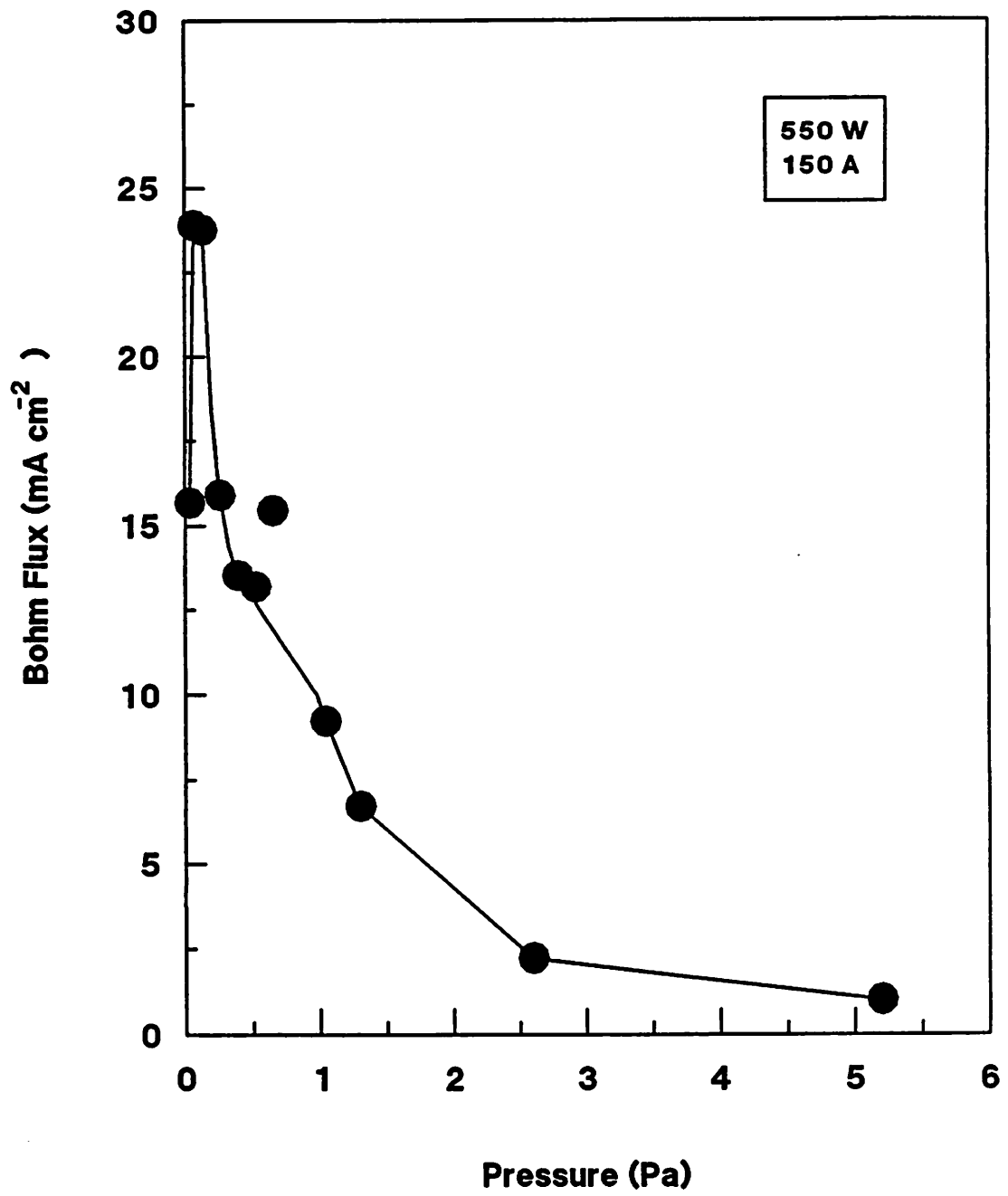


Fig. 2

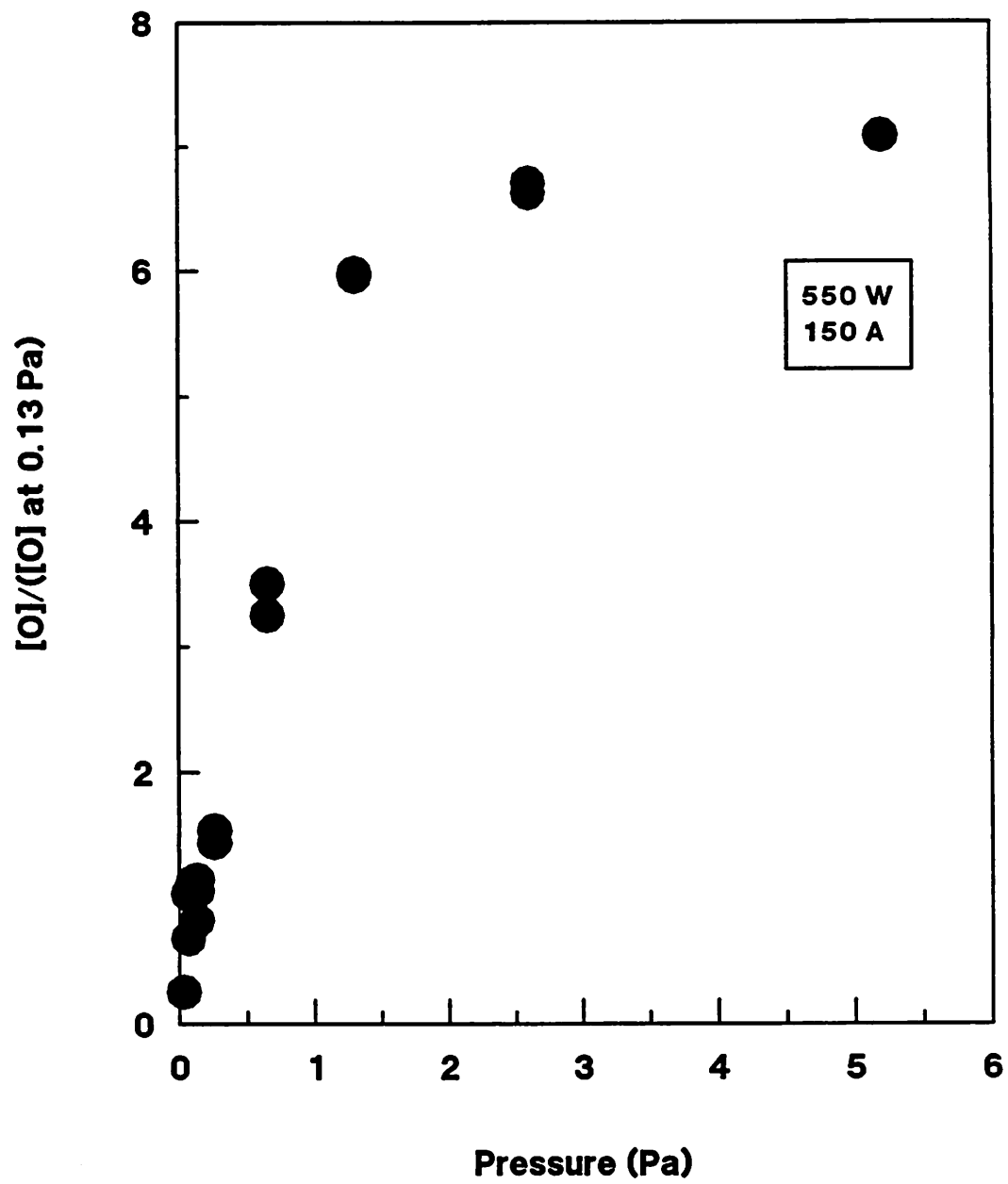


Fig. 3

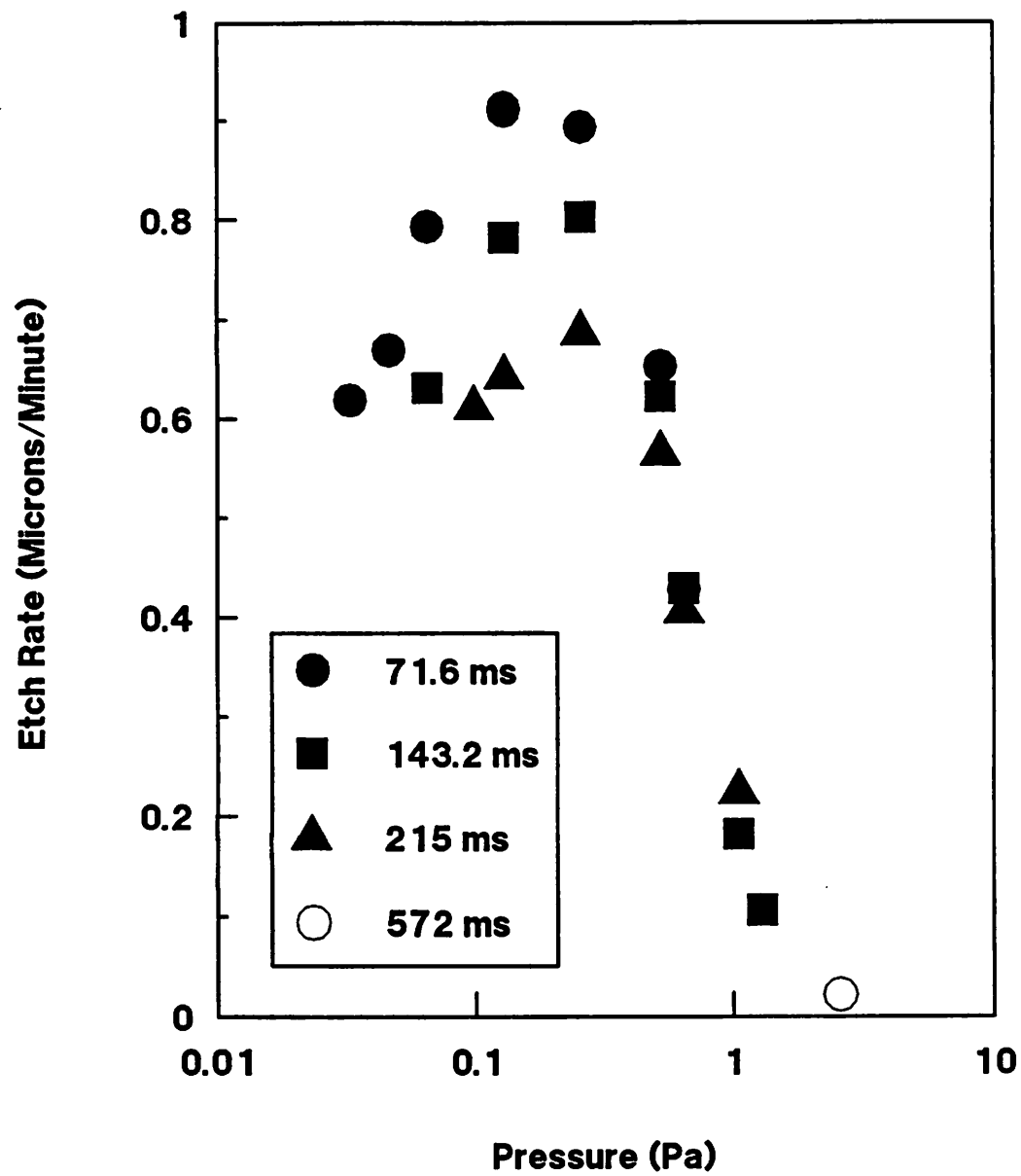


Fig. 4

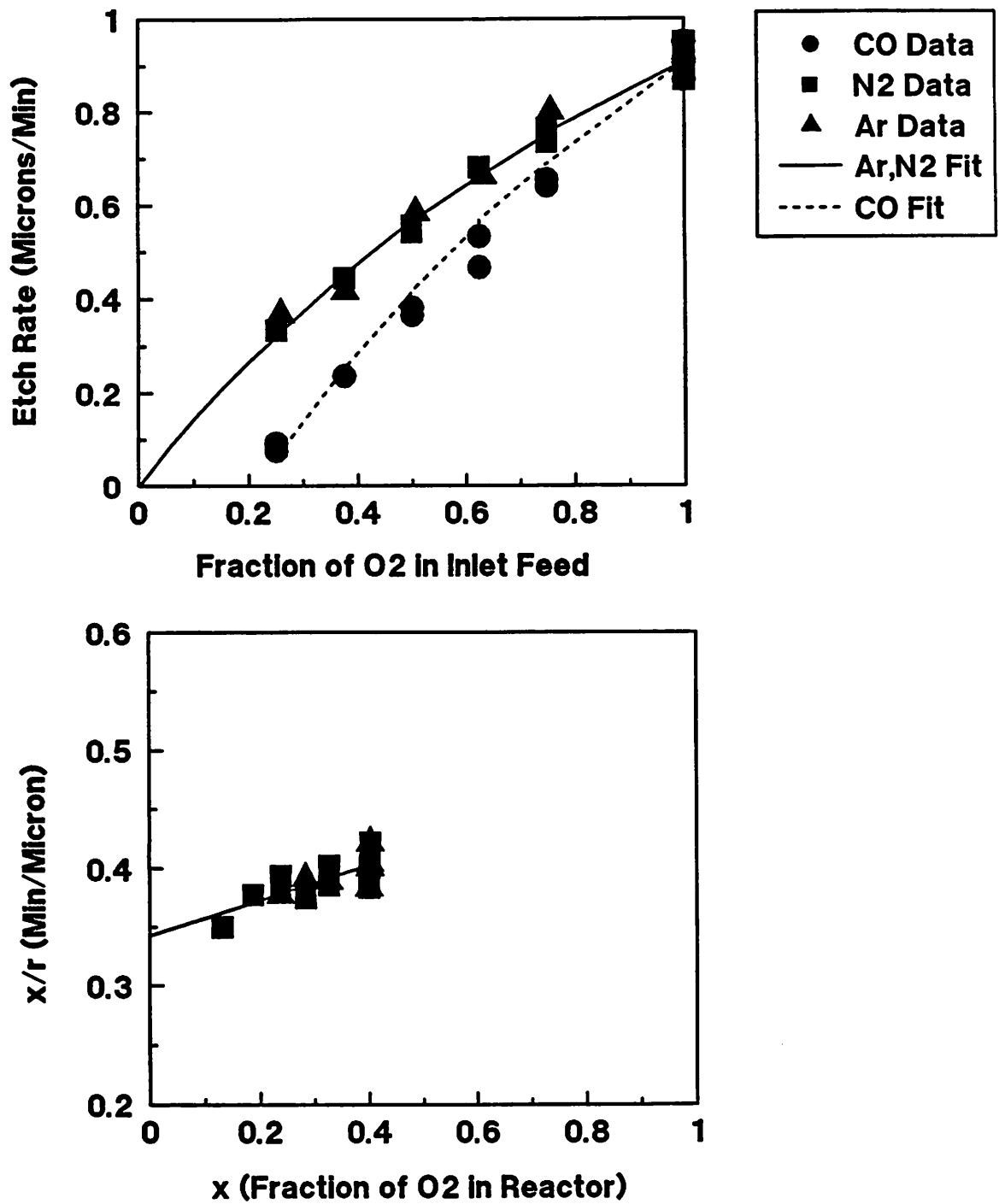


Fig. 5

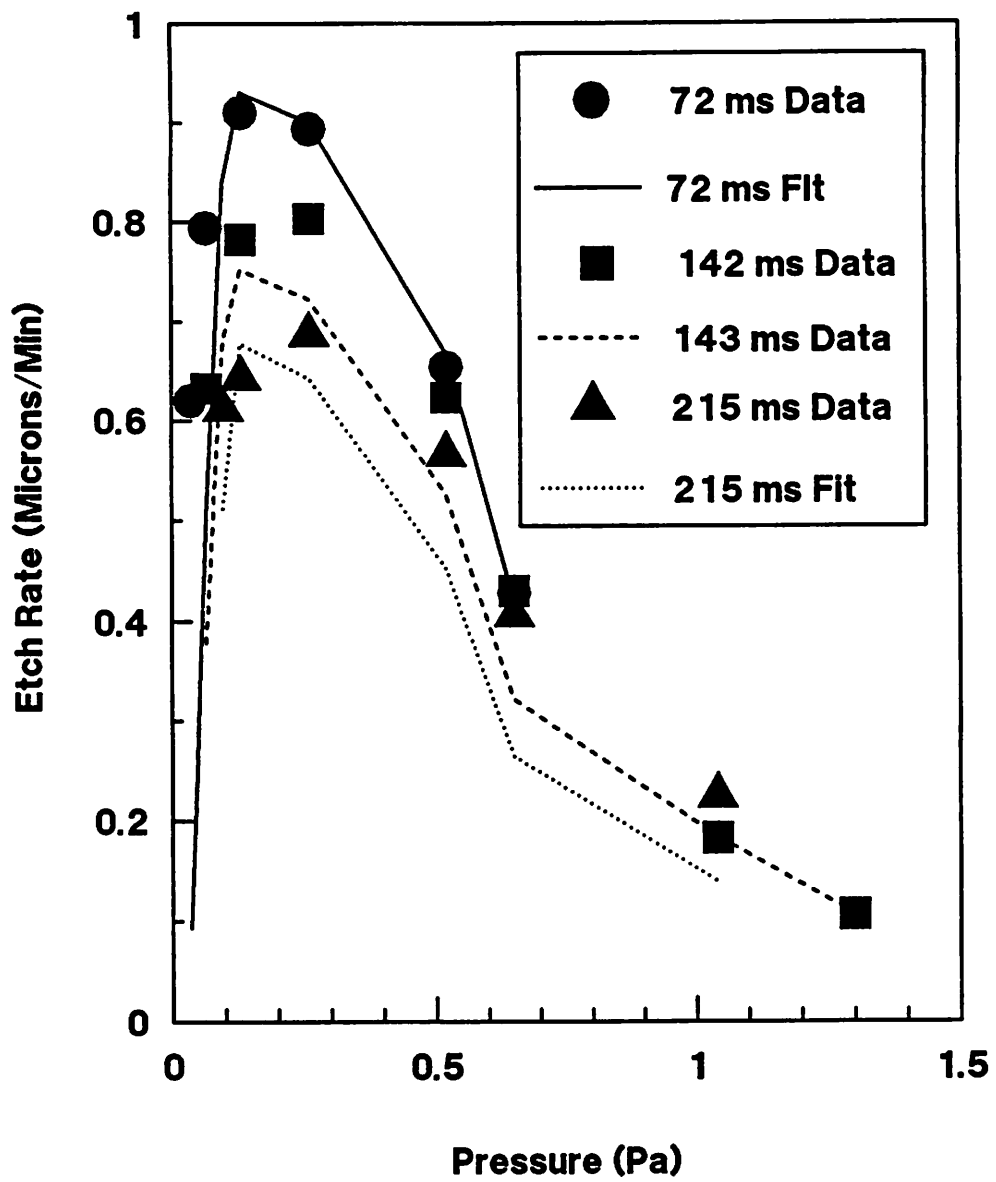


Fig. 6

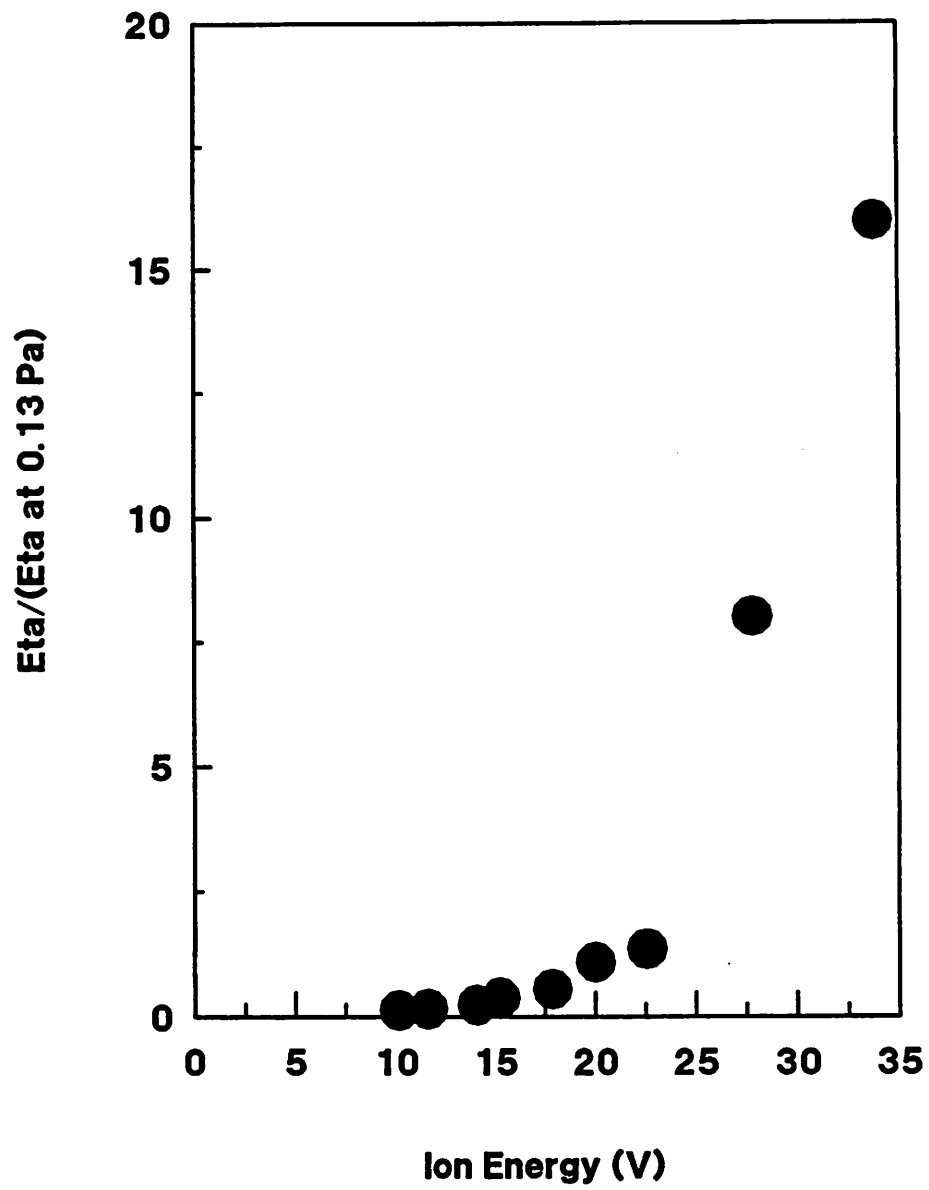


Fig. 7

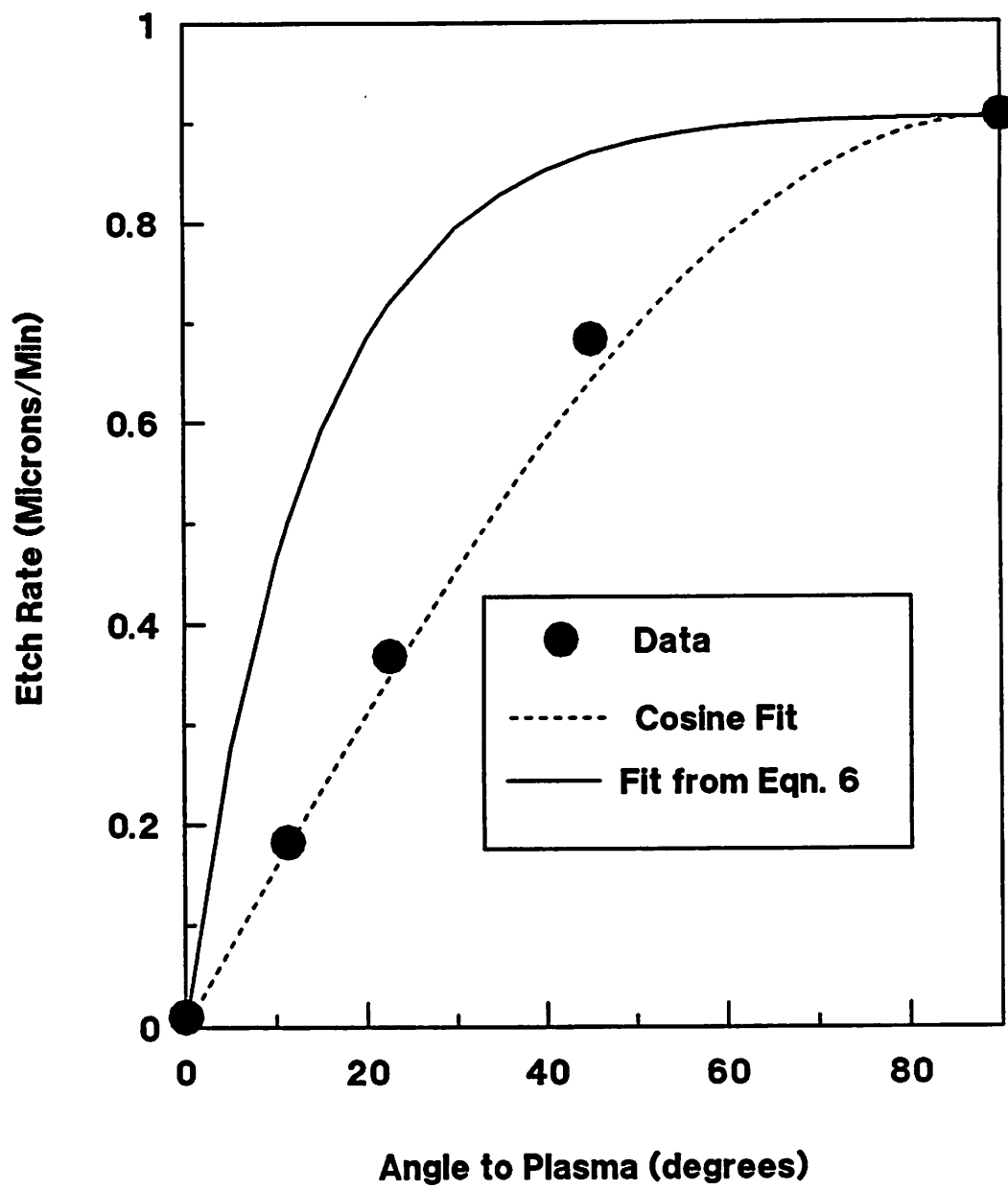
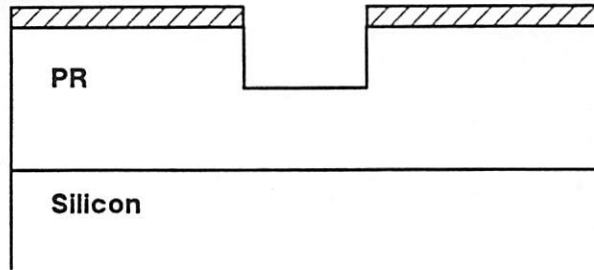


Fig. 8

Pre ECR Etch

Dielectric Mask



Post 45 Degree ECR Etch

Plasma Flux

Dielectric Mask

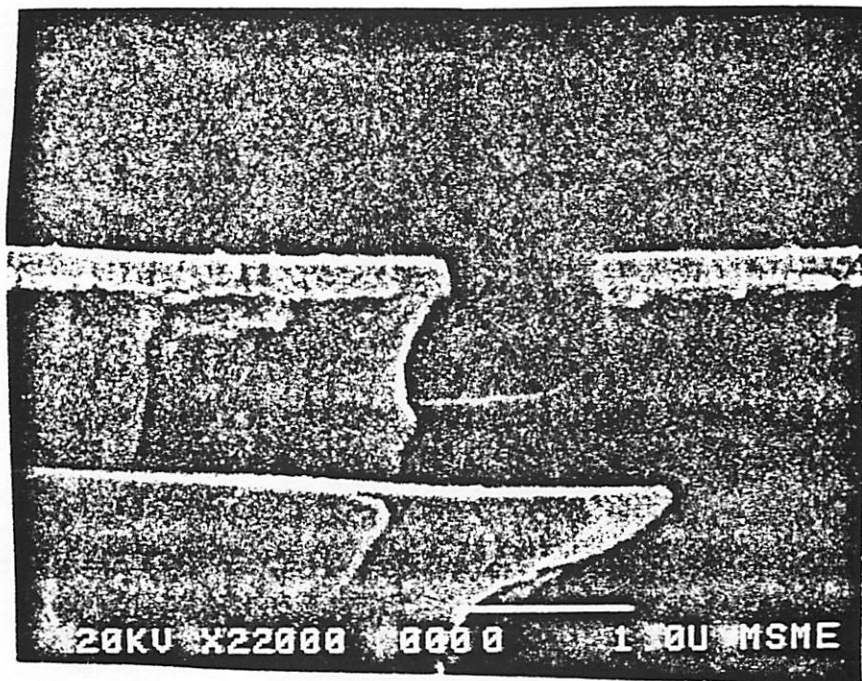
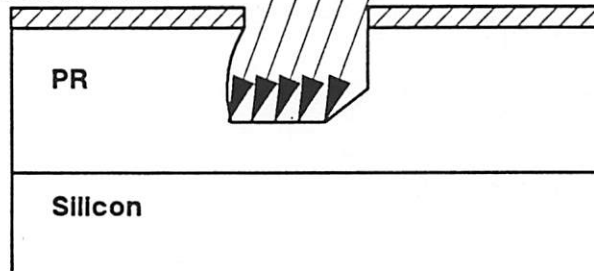


Fig. 9